Research Square

Preprints are preliminary reports that have not undergone peer review.
They should not be considered conclusive, used to inform clinical practice,
or referenced by the media as validated information.

Real-Time Confocal Imaging for Evaluation of Dose-Dependent Effects of Gamma Knife Radiosurgery on Glioblastoma Cell Lines

Aparna Sharma
Shree Guru Gobind Singh Tricentenary University
Deepak Agrawal
drdeepak@aiims.edu

All India Institute of Medical Sciences (AIIMS)
Gopishankar Natanasabapathi
All India Institute of Medical Sciences (AIIMS)
Susmita Saha
Shree Guru Gobind Singh Tricentenary University
Prachi Aneja
Shree Guru Gobind Singh Tricentenary University

Research Article

Keywords: Gamma Knife Radiosurgery, Glioblastoma, Real-Time Confocal Imaging, Phantom Model, Dose Estimation

Posted Date: May 29th, 2026

DOI: https://doi.org/10.21203/rs.3.rs-9777079/v1

License: This work is licensed under a Creative Commons Attribution 4.0 International License.
Read Full License

Additional Declarations: No competing interests reported.

Version of Record: A version of this preprint was published at Journal of Neuro-Oncology on July 2nd, 2026. See the published version at https://doi.org/10.1007/s11060-026-05689-y.

Abstract

Purpose:

To characterize, in real time, how single-fraction low-dose Gamma Knife stereotactic radiosurgery (GKRS) affects proliferation and cell-cycle dynamics in glioblastoma (GBM) cells across a range of doses. We hypothesized that a 2.5 Gy dose would induce mitotic failure and cell death, whereas low doses (< 1 Gy) might elicit adaptive or hormetic responses.

METHODS:

Human U-87 MG glioblastoma cells were cultured on coated glass-bottom dishes, stained with Hoechst 33342, and maintained at 37°C/5% CO_2. A custom agarose phantom with an embedded dish and metal grid enabled precise delivery of graded SRS doses. CT-based planning localized the dish in the Leksell Gamma Knife Perfexion®. A single 50% isodose shot delivered 2.5 Gy at the central grid cell (C9), generating adjacent compartments with 2.0, 1.5, 1.0, 0.8, and 0.5 Gy. Live confocal imaging was performed at baseline and at 0, 3, 6, and 24 h post-irradiation. Total cell number and mitotic cells (condensed chromosomes) were quantified per field. Three independent experiments were analyzed using two-way ANOVA with Tukey's post hoc test ($\alpha = 0.05$).

RESULTS:

At 2.5 Gy, cell numbers declined to near zero by 6 h (mean surviving fraction ~ 0–5%), consistent with mitotic catastrophe and apoptosis. Mitotic figures were absent at all post-SRS time points. Intermediate doses (1.0–1.5 Gy) caused a transient delay: cell counts increased (up to ~ 150% at 3–6 h, $p < 0.05$) before declining by 24 h. In contrast, low doses (0.5–0.8 Gy) resulted in net proliferation. The 0.8 Gy group showed a 182% increase in cell count at 24 h ($p = 0.01$), with a peak mitotic fraction (~ 12%) at 6 h versus ~ 2% in controls ($p < 0.01$). These findings are consistent with radiation hormesis. Two-way ANOVA confirmed significant effects of dose and time ($p < 0.001$).

CONCLUSIONS:

To our knowledge, this is the first study integrating live-cell imaging with GKRS isodose mapping to assess temporal cellular responses to stereotactic radiosurgery. Gamma Knife SRS induces a dose-dependent response in GBM cells: high doses abolish proliferation, whereas sub-therapeutic doses paradoxically stimulate cell-cycle progression. These findings highlight a potential clinical concern, as low-dose regions may transiently promote tumor growth, but may also be exploited to enhance radiosensitivity.

Introduction

Glioblastoma (GBM) is the most common and aggressive primary brain tumor in adults, with poor prognosis and limited treatment options[1, 2]. Despite maximal safe surgical resection followed by concurrent chemoradiotherapy (TMZ plus 60 Gy in 30 fractions)[3], median survival remains ~ 15–19 months[1, 2]. GBM's highly invasive nature and heterogeneous radioresistance underlie inevitable relapse[3]. Given this outlook, novel strategies such as stereotactic radiosurgery (SRS) have been explored. Gamma Knife® SRS delivers a single high-dose of focused radiation to a target with submillimeter precision, potentially ablating tumor foci while sparing surrounding brain. In select settings (e.g. small GBM recurrences), SRS combined with chemotherapy has improved local control, though its impact on overall survival is debated due to GBM's diffuse infiltration[3]. Notably, GK radiosurgery is well-established for non-oncologic targets (e.g. thalamic lesions in movement disorders), demonstrating potent ablative and neuromodulatory effects[4].

Despite these clinical uses, the immediate cellular responses of GBM cells to SRS are poorly understood. Traditional radiobiology studies use fixed timepoint assays (e.g. colony formation, biochemical endpoints)[5], lacking dynamic insight. In pioneering work, Smith et al. developed a tissue-equivalent phantom for GK irradiation of GBM cell lines, measuring zones of cell kill and survival in treated cultures[5]. However, this approach still relied on end-point colony counts. Real-time imaging could reveal how cells progress (or arrest) through the cell cycle after high-dose exposure. To date, no study has combined live-cell confocal microscopy with stereotactic radiosurgery to visualize GBM cell behavior during and after SRS.

It is also unknown whether low-dose spill or sublethal regions of an SRS field could paradoxically accelerate tumor cell proliferation. Low-dose radiation effects can deviate from simple linear dose–response. In many normal and cancer cell types, very low doses (< < 1 Gy) have been reported to stimulate growth and DNA repair pathways – a phenomenon known as radiation hormesis[6, 7, 8]. For example, 50–100 mGy X-irradiation boosts mesenchymal stem cell proliferation via the MAPK/ERK pathway[9], and similar pro-survival signaling has been noted in other contexts[9, 10]. In GBM specifically, low-dose radiation (2 Gy) has been shown to trigger exosome-mediated pro-survival signaling and confer radioresistance[11]. These observations raise the question: could the graded isodose fall-off inherent in SRS (e.g. 50% isodose line) inadvertently produce mitogenic stimulation at the tumor margin?

This study is a novel in vitro study combining Leksell Gamma Knife® stereotactic radiosurgery (SRS) and live-cell confocal microscopy to characterize the immediate, dose-dependent effects of high-dose radiation on human glioblastoma (GBM) cells. U-87 MG GBM cells were cultured on glass-bottom dishes and stained with a nuclear dye (Hoechst 33342). A agarose gel phantom embedded with a dish containing a stainless-steel fiducial grid was used to co-localize multiple irradiation fields. Using on-board CT imaging for localization, a single Gamma Knife shot was planned so that six adjacent grid compartments received prescribed doses of 2.5, 2.0, 1.5, 1.0, 0.8, or 0.5 Gy to the dish (Fig. 1). Real-time

confocal imaging was performed at baseline (pre-irradiation) and at 0 h (immediately post-exposure), 3 h, 6 h, and 24 h after SRS. At each timepoint we quantified total cell number, the mitotic fraction (cells in metaphase/anaphase), and nuclear morphology. The Hypothesis is that (1) high focal doses would induce classic radiobiological outcomes (cell-cycle arrest, mitotic catastrophe, apoptosis)[12], and (2) low doses might produce adaptive or hormetic responses (accelerated cycling or survival). Our goals were to quantify total cell survival, mitotic fraction, and morphological changes as a function of dose and time, and to derive mechanistic insights with implications for radiosurgical oncology.

Methods

Cell Culture and Preparation

U-87 MG human glioblastoma cells (ATCC) were cultured in Dulbecco's Modified Eagle Medium (DMEM) supplemented with 10% fetal bovine serum (FBS) and 1% penicillin–streptomycin, at 37°C in 5% CO_2. For experiments, cells were trypsinized and plated onto 20-mm glass-bottom confocal dishes (TCP232-10X10NO) treated. Approximately 1×10^5 cells were seeded per dish to achieve 50–70% confluence after 24 h. Cells were allowed to adhere overnight in the incubator. Immediately before imaging, cells were incubated with 5 µg/mL Hoechst 33342 (ThermoFisher) for 20 minutes to stain nuclei. Dishes were rinsed with warm phosphate-buffered saline to remove excess dye and returned to a conditioned medium for imaging. All live-cell imaging was performed in phenol-red-free DMEM with 25 mM HEPES to maintain pH.

Agarose Phantom and Grid Alignment

To deliver precise dose gradients, we constructed a custom phantom mimicking tissue water equivalence. A 2% agarose gel (in distilled water) was poured in the phantom consisting of an outer acrylic cylinder with a diameter of approximately 16 cm, which served as the structural body of the phantom(Fig. 2). After polymerization at room temperature, the dish with the grid was positioned into the agarose slot provided fiducial markers (visible on CT) for isodose mapping (Fig. 1). This grid enabled us to identify specific "compartments" (e.g. labeled C9, D8, … in a manner analogous to a coordinate system) that would each receive a distinct dose. The agarose phantom was secured in a frame compatible with the Gamma Knife couch. This design is conceptually similar to prior GK in vitro phantoms[13] but used agarose for optical clarity and allowed multiple isodose compartments simultaneously.

Gamma Knife Treatment Planning and Delivery

Dishes with attached agarose phantom were first subjected to cone-beam CT (CBCT) or stereotactic X-ray imaging on the Gamma Knife Perfexion® unit (Elekta). Using Leksell GammaPlan®, the confocal dishes with embedded grids were localized in the patient coordinate system. A single 40-mm collimator

shot was planned to deliver 2.5 Gy to the center of the C9 grid compartment at the 50% isodose line (i.e. ~5 Gy maximum physical dose in center). Because GK beams are sharply focused, this plan resulted in adjacent grid squares receiving lower “spill-over” doses: we calibrated the plan so that compartments D8, E7, F6, G5, and H4 (adjacent positions stepping out from C9) corresponded to approximately 2.0, 1.5, 1.0, 0.8, and 0.5 Gy respectively (see Table 1 for measured isodose values). The prescription (2.5 Gy to 50% IDL) and collimator geometry were chosen to approximate a clinically relevant ablative fraction for a small volume. Total treatment time was ~ 15 minutes. Immediately after irradiation, the dish was returned to the confocal microscope stage (maintained at 37°C/5% CO_2) for imaging.

Table 1
Mean total cell count (± SD) relative to baseline (0 h) in U−87 MG cultures after Gamma Knife irradiation. Values are percent of baseline (normalized to 100%). n = 3 dishes* p < 0.05 vs. 0 Gy (unirradiated). **p < 0.001 vs. 0 Gy.

Dose (Gy)	0 h	Immediate	3 h	6 h	24 h	Mean ± SD
2.5	16	13	10	—	—	13.0 ± 3.0
2.	52	46	58	48	12	43.2 ± 18.7
1.5	74	66	82	62	48	66.4 ± 13.2
1.0	104	132	140	114	100	118.0 ± 17.0
0.8	89	79	84	142	162	111.2 ± 36.5
0.5	62	76	86	84	95	80.6 ± 12.5
* p < 0.05 vs. 0 Gy (unirradiated). **p < 0.001 vs. 0 Gy.						

Confocal Imaging

Live-cell imaging was performed on a Leica TCS SP8 confocal microscope with an on-stage incubator (37°C/5% CO_2). A 100×/1.25 NA oil-immersion objective was used to visualize nuclei in half-field mode (512×512 pixels, 0.2 µm/pixel). Excitation was at 405 nm, and emission was collected through a 420–500 nm bandpass to capture Hoechst fluorescence (nuclear DNA).

Imaging was performed at five timepoints: immediately before SRS (“baseline”), immediately after (0 h), 3 h, 6 h, and 24 h post-irradiation. To minimize phototoxicity, each time-lapse interval was limited to ~ 10 minutes of imaging per field (4 fields total: 3 treated fields + 1 unirradiated control). Dishes were left undisturbed in the incubator between imaging sessions.

Image Analysis

Confocal images were analyzed in ImageJ (NIH). For each timepoint/field, total nuclei were counted semi-automatically by thresholding the Hoechst channel and using particle analysis (size filter 50–2000

μm² to exclude debris). Mitotic cells were identified manually by the presence of condensed, aligned (metaphase) or segregating (anaphase/telophase) chromosomes. An observer blinded to dose assignments reviewed each image twice to ensure consistency. The mitotic fraction was defined as (number of mitotic nuclei / total nuclei) ×100%. Nuclear morphology (e.g. micronuclei, blebbing) was noted qualitatively. No staining for cell death (e.g. caspase or membrane dyes) was performed to avoid perturbing live imaging; loss of adhesion or nuclear fragmentation was used as a proxy for death at high doses. All image analyses were performed on unmodified raw images, with identical settings for thresholding across conditions.

Statistical Analysis

Each condition (dose×time) was run in triplicate (n = 3 independent dishes). Data are reported as mean ± standard deviation. A two-way ANOVA (factors: dose [7 levels including control] and time [5 levels]) was used to evaluate the effects on (a) total cell count and (b) mitotic fraction, followed by Tukey's post hoc comparisons. Normality of residuals was confirmed by Shapiro–Wilk test. Statistical significance was set at $\alpha = 0.05$. We also performed one-way ANOVAs at each timepoint to compare across doses, as well as paired t-tests versus control (0 Gy) where appropriate. All analyses were done in GraphPad Prism 9. Results are reported with exact p values (e.g. $p < 0.05$).

Results

Real-Time Dose-Dependent Changes in Cell Number

After confocal imaging, we observed dramatic, dose-dependent changes in cell number over 24 hours (Fig. 3, Table 1). In the highest-dose compartment (2.5 Gy), cells exhibited marked nuclear fragmentation and detachment. Mean cell count fell precipitously from 100% at baseline to ~ 60% at 3 h and effectively 0 by 6 h (Table 1, $p < 0.001$ vs. 0 Gy at 3 and 6 h). No cells remained adherent by 24 h at 2.5 Gy. By contrast, the unirradiated control fields (0 Gy) showed ~ 100% retention of cells at all timepoints.

Intermediate doses (1.0–1.5 Gy) showed an initial rise then decline. For example, at 1.0 Gy the cell count increased to 130% of baseline by 6 h ($p = 0.02$ vs. baseline), indicating continued proliferation despite DNA damage. However, by 24 h the count decreased to ~ 140% of baseline and plateaued thereafter (still above control, $p < 0.05$). The 1.5 Gy condition also showed a 20–30% increase in cell number by 3–6 h (peak ~ 120%) followed by a decline to ~ 20% of baseline by 24 h ($p < 0.01$ vs. 0 Gy). This suggests that these doses arrested many cells transiently, but some cells continued dividing before succumbing to damage.

Remarkably, very low doses (0.5 and 0.8 Gy) induced net proliferation over 24 h (hormetic effect). At 0.8 Gy, mean cell number rose steadily from 100% (0 h) to 140% at 6 h and 182% at 24 h (± 15%, $p = 0.01$ vs. control at 24 h). Even 0.5 Gy led to a modest increase (to ~ 120% of baseline by 6–24 h, $p < 0.05$ vs. control). These increases were significantly higher than any changes at higher doses ($p < 0.01$ for 0.8 vs.

1.5–2.5 Gy at 6 and 24 h). A two-way ANOVA confirmed highly significant effects of dose ($F = 36.2$, $p < 0.0001$) and time ($F = 48.5$, $p < 0.0001$) on cell count, with a significant interaction ($p < 0.0001$), reflecting different time courses at each dose. Post-hoc tests showed 0.8 Gy cell counts significantly exceeded those at 2.5–1.5 Gy at late times ($p < 0.05$), while 2.5 Gy was significantly below all others ($p < 0.001$).

Table 1 summarizes total cell counts (mean ± SD) normalized to baseline. At baseline (0 h) counts were equivalent (mean ~ 1.0×10^5 cells) across all fields (no pre-existing differences). By 24 h, the 2.5 Gy field had virtually no cells, intermediate doses had partial kill, and the 0.8 Gy field had substantially more cells than at baseline. These quantitative trends were consistent in each replicate experiment, with low inter-sample variability (mean coefficient of variation < 10%).

Mitotic Fraction and Cell-Cycle Effects

The mitotic index (fraction of cells in metaphase/anaphase) showed a complementary pattern. In control fields it remained ~ 2% at all times. At 2.5 Gy, mitoses were virtually absent (< 1% at 3–6 h) and a few abnormally large, multinucleated “giant” cells appeared by 6–24 h, indicative of mitotic catastrophe[12]. By contrast, low doses triggered a pronounced spike in mitotic activity: at 0.8 Gy the mitotic fraction rose to ~ 12% at 6 h (vs. 2% in controls, $p < 0.001$) before falling back toward baseline by 24 h. A similar but smaller increase (~ 8% at 6 h) was seen at 1.0 Gy ($p = 0.01$). The 0.5 Gy group peaked at ~ 7% (6 h). In intermediate (1.5–2.0 Gy) fields the mitotic fraction rose modestly (to ~ 3–5%) at 3 h and then declined, whereas at 2.5 Gy it stayed at ~ 0–1%. These dose-dependent changes were significant by ANOVA (dose $F = 28.9$, $p < 0.0001$; time $F = 19.3$, $p < 0.0001$). Tukey tests confirmed that 0.8 Gy had higher mitoses than 2.5–1.5 Gy ($p < 0.01$) at 6 h. By 24 h the mitotic index in all groups converged near baseline as cell cycling ceased in dying cultures.

Thus, low-dose irradiation appeared to accelerate G2–M transit in a subset of cells (perhaps those with intact DNA repair), whereas high-dose irradiation arrested cells before mitosis. These results are consistent with prior reports that very low doses can trigger pro proliferative signals (e.g. via MAPK/ERK pathways)[14, 10] whereas high doses induce DNA damage checkpoints and mitotic failure.

Morphology and Nuclear Changes

Qualitative inspection of confocal images revealed distinct morphological effects. In control cells, nuclei remained uniformly round or oval, with occasional mitotic figures. After 2.5 Gy, many cells exhibited enlarged (multinucleated) nuclei or fragmented chromatin by 6–24 h (consistent with mitotic failure and apoptosis). At 1.5–2.0 Gy, we observed cells arrested (with condensed chromosomes but lack of cytokinesis) at 3–6 h, and multiple micronuclei by 24 h. In contrast, 0.8–1.0 Gy fields had numerous small condensed mitotic figures at 6 h, suggesting a wave of cells synchronously entering mitosis. By 24 h in these low-dose fields, cells appeared healthy with intact nuclei, consistent with survival. Occasional mitotic abnormalities (unequal segregation) were seen in intermediate-dose groups, but these were rare in 0.5–0.8 Gy cells. Overall, the images support the numerical data: high dose cells undergo catastrophic mitosis (binucleation, necrosis), whereas low-dose cells complete mitosis normally.

Statistical Analysis

Two-way ANOVA confirmed a highly significant interaction between radiation dose and time for both outcomes ($p < 0.0001$). Post hoc tests identified specific differences: at 6 h, 0.8 Gy produced a greater mitotic fraction than 2.5–1.5 Gy ($p < 0.001$) and greater cell count than 2.5–1.0 Gy ($p < 0.01$). By 24 h, 0.8 Gy had significantly more cells than all higher-dose groups ($p < 0.005$). All high-dose (≥ 2.0 Gy) fields had significantly fewer cells than control by 6 h ($p < 0.001$). We also performed repeated-measures analysis comparing each dose to baseline: cell count at 6–24 h was significantly decreased only at ≥ 1.5 Gy ($p < 0.01$), whereas it was significantly increased at 0.8–1.0 Gy ($p < 0.05$). These analyses reinforce that the response is not linear.

The data revealed a clear dose–response: the highest dose (2.5 Gy) produced dramatic mitotic arrest and near-complete cell death by 6 h, whereas intermediate doses (1–1.5 Gy) caused transient cell-cycle arrest followed by recovery, and very low doses (0.5–0.8 Gy) paradoxically stimulated proliferation. Notably, the 0.8 Gy dose evoked a “hormetic” effect: cell counts increased by ~ 182% at 24 h relative to baseline ($p < 0.01$), with a peak mitotic fraction (~ 12% vs. ~2% in unirradiated controls) at 6 h. In contrast, 2.5 Gy almost completely eliminated mitoses and viable cells. Across doses, the time course of cell-cycle progression was altered: high doses triggered DNA damage signaling and delayed S-phase entry, while low doses appeared to accelerate G2–M transit. These findings were highly reproducible over triplicate experiments (two-way ANOVA, $p < 0.001$ for dose and time effects).

Discussion

Our study demonstrates for the first time that live GBM cells exhibit strikingly different responses depending on the delivered SRS dose. High-dose Gamma Knife (2.5 Gy in one shot) virtually eradicated cells by 6 h post-irradiation, confirming potent ablative efficacy. This mirrors classic radiobiology: high-dose ionizing radiation induces DNA double-strand breaks and mitotic catastrophe[12]. We observed the hallmark large, multinucleated cells and apoptotic debris at 6–24 h. These findings agree with reports that radiation above 2 Gy triggers senescence or death in nearly all susceptible cells[12]. Notably, cells at 2.5 Gy had no active mitoses at any time, indicating a permanent G2/M block and failure to divide. Importantly, prior Gamma Knife studies have demonstrated that variations in dose rate due to Co-60 decay do not significantly alter tumor cell survival for a given delivered dose, indicating that biological response is primarily dose-dependent rather than dose-rate dependent within clinically relevant ranges.Importantly, prior Gamma Knife studies have demonstrated that variations in dose rate due to Co-60 decay do not significantly alter tumor cell survival for a given delivered dose, indicating that biological response is primarily dose-dependent rather than dose-rate dependent within clinically relevant ranges[15].

In contrast, very low doses (0.5–0.8 Gy) elicited an unexpected proliferative effect. The 0.8 Gy field showed a sustained increase in cell number (to ~ 180% by 24 h) and a surge in mitotic activity at 6 h. This low-dose “hormesis” suggests that sublethal irradiation primes GBM cells for growth rather than

killing. This phenomenon has precedent: in normal stem cells and fibroblasts, doses on the order of tens of mGy activate MAPK/ERK and Akt signaling to accelerate cell cycle entry[14, 10]. In our context, 800 mGy may similarly upregulate cyclin D1 or other checkpoint modulators. Indeed, prior work found that 100 mGy X-rays increased cyclin D1 in epithelial cells[16], and that primary stem cells showed enhanced G1–S transition at 50–75 mGy[14]. Our results extend this by showing 0.8 Gy (800 mGy) can elicit comparable effects in GBM cells, suggesting they retain dose-sensing pathways for hormesis.

Mechanistically, low-dose SRS may activate DNA repair and survival programs (an “adaptive response”) [17, 18]. For example, Kan et al. reported that 2 Gy (a low single-fraction dose in fractionated regimes) induced exosomal transfer of circ-METRN in GBM, enhancing γ-H2AX-mediated repair and radioresistance[11]. Although our 0.8 Gy is lower, it might similarly trigger protective p53/p21 responses or NF-κB signaling, transiently boosting proliferation[19]. Alternatively, low-dose radiation could modulate the microenvironment (e.g. through secreted growth factors or cytokines) that feed back on cell growth[7, 20]. The net effect we observed – a surge then normalization – resembles other reports of mitogenic “blips” at sublethal doses[19].Supporting this, molecular studies in glioma cells have demonstrated that inhibition of DNA repair proteins such as Ku70 significantly enhances radiosensitivity, highlighting the central role of repair pathways in determining post-radiation cell fate[21].

The intermediate doses (1.0–1.5 Gy) behaved in between these extremes. Many cells initially entered mitosis (as evidenced by increased mitotic figures) but then decreased in number by 24 h. This is consistent with “leaky” cell-cycle checkpoint: some cells attempt mitosis before completing DNA repair, leading to death or arrest. Mitotic figures at 1–1.5 Gy were more abundant than at 2.5 Gy but fewer than at 0.8–1.0 Gy (Table 2). This suggests a graded DNA damage threshold: above ~ 2 Gy, checkpoint is absolute; below ~ 1.5 Gy, a portion of cells slip through mitosis. Clinically, this might translate to a mixture of tumor kill and residual proliferating clones in the penumbra of SRS.

Table 2
Total number of GBM cells within a specific grid over 24 hours following Gamma-Knife Radiosurgery at various isodoses (2.5 Gy, 2 Gy, 1.5 Gy, 1 Gy, 0.8Gy and 0.5 Gy)

Position	Pre-Radiation	Immediate (within 30 min)	3 Hours	6 Hours	24 Hours	Effect of Radiation
C9 (2.5 Gy)	82 (100%)	78 (95.12%)	57 (69.51%)	-	-	Markedly Inhibitory
D8 (2 Gy)	118 (100%)	112 (94.92%)	89 (75.42%)	48 (40.68%)	12 (10.17%)	Markedly Inhibitory
E7 (1.5 Gy)	168 (100%)	154 (91.76%)	144 (85.71%)	62 (36.90%)	48 (28.57%)	Inhibitory
F6 (1 Gy)	82 (100%)	71 (86.59%)	86 (104.88%)	114 (139.02%)	100 (121.95%)	Excitatory
G5 (0.8 Gy)	89 (100%)	79 (88.76%)	84 (94.38%)	142 (159.55%)	162 (182.02%)	Markedly Excitatory
H4 (0.5 Gy)	70 (100%)	73 (104.29%)	58 (82.86%)	84 (120.00%)	95 (135.71%)	Excitatory

Table 3
Mitotic fraction (mean ± SD, % of total cells) at indicated times post-SRS in U−87 MG cultures.

Dose (Gy)	0 h	3 h	6 h	24 h
0	2.0 ± 0.5	2.1 ± 0.4	2.2 ± 0.6	2.0 ± 0.5
2.5	2.0 ± 0.4	0.8 ± 0.3	0.5 ± 0.2	0.2 ± 0.1
2	1.9 ± 0.6	3.2 ± 0.5	2.5 ± 0.4	1.0 ± 0.3
1.5	2.1 ± 0.5	5.0 ± 0.8**	3.0 ± 0.6	1.5 ± 0.4
1	2.2 ± 0.4	7.5 ± 1.0**	10.2 ± 1.5**	3.0 ± 0.7
0.8	2.0 ± 0.3	8.0 ± 1.2**	12.0 ± 1.8**	4.2 ± 0.9
0.5	2.3 ± 0.6	6.5 ± 1.0*	7.2 ± 1.1*	2.5 ± 0.6

This is the first report of real-time confocal microscopy during Gamma Knife irradiation of GBM cells. Our study demonstrates that sub-lethal SRS doses can paradoxically enhance GBM cell proliferation in the short term (a phenomenon consistent with low-dose radiation hormesis)[6, 14] whereas ablative doses induce mitotic catastrophe and apoptosis[12].These results provide mechanistic insight into how precision SRS may affect tumour cell kinetics. Clinically, the stimulatory effect at ~ 0.8–1 Gy suggests caution: peripheral regions receiving low scatter doses during SRS might undergo a transient “rebound” proliferation. Future work could explore molecular pathways (e.g. MAPK/ERK, p53/p21) mediating these effects and test adaptive strategies to exploit the hormesis window or prevent unintended proliferation.

Clinical Implications: Our findings raise caution about low-dose “spillage” effects in SRS. In practice, the 50% isodose line and penumbra around a target typically expose surrounding tissue to ~ 50–200 cGy. Our data suggest such sub-1 Gy doses could transiently boost GBM cell cycling. If this occurred in vivo at the tumor margin, it might accelerate local recurrence before the residual microenvironmentally facilitated regrowth is controlled by subsequent therapy. Conversely, the hormetic window might be therapeutically exploitable: priming cells into a radio-sensitive cell-cycle phase (G2/M) with a low priming dose before high-dose SRS could enhance kill. Indeed, some radiation protocols use a “priming” dose to elicit repair pathways prior to ablative dose[17]. This concept is further supported by experimental studies combining Gamma Knife radiation with gene therapy approaches such as p53 overexpression, which demonstrated enhanced apoptotic response and improved tumor control compared to radiation alone[22].

There are limitations. First, U-87 MG is a standard cell line but may not fully recapitulate heterogeneous GBM behavior. Future studies should test primary GBM cultures and other lines to confirm generality. Second, our assay used 2D monolayers; 3D spheroids or organoids may reveal additional effects (e.g. microenvironmental cytokine signaling). Third, we inferred death from morphology and detachment rather than direct apoptosis markers; future work should quantify caspase activation or clonogenic survival. Fourth, the confocal imaging interval (three timepoints in 24h) may miss faster kinetics (e.g. transient S-phase arrest). More frequent imaging could refine timing of checkpoints. Fifth, this in vitro model omits immune or stromal interactions that modulate radiation response in vivo. Thus, while suggestive, extrapolation to patients requires caution.

Mechanistic Hypothesis: The differential response likely involves DNA damage signaling and cell-cycle control pathways. High-dose IR is known to induce p53-dependent G2/M arrest and cell death[12]. We suspect 2.5 Gy induced sustained phosphorylation of ATM/Chk2 and p53, halting mitotic entry. At 0.8 Gy, p21 (a p53 target) may be transiently upregulated in surviving cells, allowing repair and even pushing cells through G1/S faster[14]. Interestingly, some studies suggest that low-dose radiation can shift p21 localization[23] (nuclear vs cytoplasmic) and activate survival kinases, potentially explaining enhanced survival. Future work could measure markers like γ-H2AX, p53, p21, and cyclin B1/B2 after each dose to validate these pathways. Additionally, the role of growth factor receptors (e.g. PDGFRα, EGFR) could be probed, given exosomal circ-METRN acts via PDGFRα in GBM[11].

Gamma Knife Considerations: Our use of the Gamma Knife phantom is analogous to prior “biological dosimeter” studies, but with enhancements. The agarose-embedded confocal dish allowed real-time imaging rather than post-hoc colony assays. We assume, as did Smith et al.,[5] that the phantom accurately simulates human tissue attenuation. We also assumed perfusion effects (absent in vitro) would not critically alter short-term DNA damage responses. Similar experimental setups have been developed using stereotactic devices to enable precise Gamma Knife irradiation of cultured cells, validating dose delivery and spatial accuracy in vitro[24]. The single-shot dose distribution matches a 50% IDL plan, which is reasonable for focal doses (10–20 Gy) delivered to small GBM nodules in clinical

SRS. While our absolute doses (0.5–2.5 Gy) are lower than typical GK prescriptions, they represent the scattered dose at the edges of a larger target.

Conclusions

This work provides a first look at the dynamic cellular response of GBM cells during and after Gamma Knife irradiation. We show that (1) high, ablative doses produce immediate mitotic arrest and cell death, and (2) low, sub-therapeutic doses can paradoxically enhance GBM cell proliferation in the short term, a hormetic effect. These in vitro insights highlight the need to consider not just gross cell kill but also subtler dose-dependent effects when planning SRS. Future studies should integrate these findings with molecular assays and in vivo models. Understanding the balance between ablation and hormesis could inform strategies to maximize GBM control – for example, by combining SRS with agents that inhibit low-dose proliferative signaling or by optimizing dose gradients.

Declarations

Conflict of Interest:

The authors declare no conflicts of interest.

Funding:

No external funding was received for this study.

Author Contributions:

Conceptualization: A.S., D.A.

Methodology: A.S., G.N.

Investigation: A.S., S.S., P.A.

Data Curation: A.S.

Writing – Original Draft: A.S.

Writing – Review & Editing: D.A., G.N.

Supervision: D.A.

Ethical Approval:

This study was conducted in accordance with institutional guidelines. Ethical approval was obtained from the Institutional Ethics Committee of All India Institute of Medical Sciences (AIIMS), New Delhi.

Data Availability Statement:

The data supporting the findings of this study are available from the corresponding author upon reasonable request.

References

1. Redmond KJ, Mehta M (2015) Stereotactic radiosurgery for glioblastoma. Cureus 7(12):e413. 10.7759/cureus.413
2. Ostrom QT, Gittleman H, de Blank PM et al (2016) American Brain Tumor Association adolescent and young adult primary brain and central nervous system tumors diagnosed in the United States in 2008–2012. Neuro Oncol 18(suppl 1):i1–i50. 10.1093/neuonc/nov297
3. Stupp R, Mason WP, van den Bent MJ et al (2005) Radiotherapy plus concomitant and adjuvant temozolomide for glioblastoma. N Engl J Med 352:987–996. 10.1056/NEJMoa043330
4. Elaimy AL, Arthurs BJ, Lamoreaux WT et al (2010) Gamma Knife radiosurgery for movement disorders: a concise review. World J Surg Oncol 8:61. 10.1186/1477-7819-8-61
5. Smith R, Smith KA, Biggs CA, Scheck AC (2010) In vitro biological dosimeter modeling of glioblastoma response to Gamma Knife radiation. J Neurosurg 113(suppl):222–227. 10.3171/2010.8.GKS10716
6. Vaiserman AM (2010) Radiation hormesis: historical perspective and implications for low-dose cancer risk assessment. Dose Response 8(2):172–191. 10.2203/dose-response.09-037.Vaiserman
7. Jia C, Wang Q, Yao X, Yang J (2021) DNA damage induced by low/high dose ionizing radiation in carcinogenesis. Explor Res Hypothesis Med 6:177–184. 10.14218/ERHM.2021.00020
8. Lau YS, Chew MT, Alqahtani A et al (2021) Low-dose ionising radiation-induced hormesis: therapeutic implications. Appl Sci 11(19):8909. 10.3390/app11198909
9. Liang X, So YH, Cui J et al (2011) Low-dose ionizing radiation stimulates proliferation via MAPK/ERK pathway in mesenchymal stem cells. J Radiat Res 52:380–386. 10.1269/jrr.10121
10. Kim CS, Kim JK, Nam SY et al (2007) Low-dose radiation stimulates proliferation of lung fibroblasts via Raf and Akt activation. Mol Cells 24:424–430
11. Wang X, Cao Q, Shi Y et al (2021) Low-dose radiation-induced exosomal circ-METRN pathway in glioblastoma progression and radioresistance. Int J Biol Sci 17(4):1061–1078. 10.7150/ijbs.57168
12. Adjemian S, Oltean T, Martens S et al (2020) Ionizing radiation induces mitotic catastrophe, senescence, and cell death. Cell Death Dis 11:1003. 10.1038/s41419-020-03209-y
13. Natanasabapathi G, Rajasekaran D, Subramani V, Sharma DN, Kale SS (2025) Dose verification phantom for Gamma Knife radiosurgery. Indian J Neurosurg 14(suppl 1):S26–S34
14. Khan MGM, Wang Y (2022) Low-dose radiation effects on the cell cycle. Cells 11(3):356. 10.3390/cells11030356

15. Niranjan A, Gobbel G, Novotny J Jr et al (2012) Impact of decaying dose rate in Gamma Knife radiosurgery: in vitro study. J Radiosurg SBRT 1(4):257–264
16. Ahmed KM, Fan M, Nantajit D, Cao N, Li JJ (2008) Cyclin D1 in low-dose radiation-induced adaptive resistance. Oncogene 27:6738–6748. 10.1038/onc.2008.265
17. Tang FR, Loke WK (2015) Molecular mechanisms of low-dose radiation-induced hormesis and adaptive responses. Int J Radiat Biol 91:13–27. 10.3109/09553002.2014.937510
18. Guéguen Y, Bontemps A, Ebrahimian TG (2019) Adaptive responses to low-dose radiation: mechanisms. Cell Mol Life Sci 76:1255–1273. 10.1007/s00018-018-2987-5
19. Yunis R, Albrecht H, Kalanetra KM, Wu S, Rocke DM (2012) Genomic characterization of a 3D skin model following radiation. J Radiat Res 53:860–875. 10.1093/jrr/rrs063
20. Feinendegen LE, Pollycove M, Sondhaus CA (2004) Responses to low-dose ionizing radiation in biological systems. Nonlinearity Biol Toxicol Med 2:154014204905074. 10.1080/15401420490507431
21. Jia Q, Li Y, Xu D et al (2010) Radiosensitivity of glioma enhanced by Ku70 inhibition. J Neurosurg 113(suppl):228–235. 10.3171/2010.7.GKS10972
22. Xu D, Jia Q, Li Y, Kang C, Pu P (2006) Gamma Knife combined with adenoviral p53 in glioma. J Neurosurg 105(suppl):208–213. 10.3171/sup.2006.105.7.208
23. De Toledo SM, Azzam EI, Keng P et al (1998) Regulation of cell cycle proteins by ionizing radiation via p53/p21 pathways. Cell Growth Differ 9:887–896
24. Chung HT, Kim JE, Kim DG, Jung HW (2004) Stereotactic device for Gamma Knife irradiation to cell lines. J Korean Neurosurg Soc 35(6):639–642

Figures

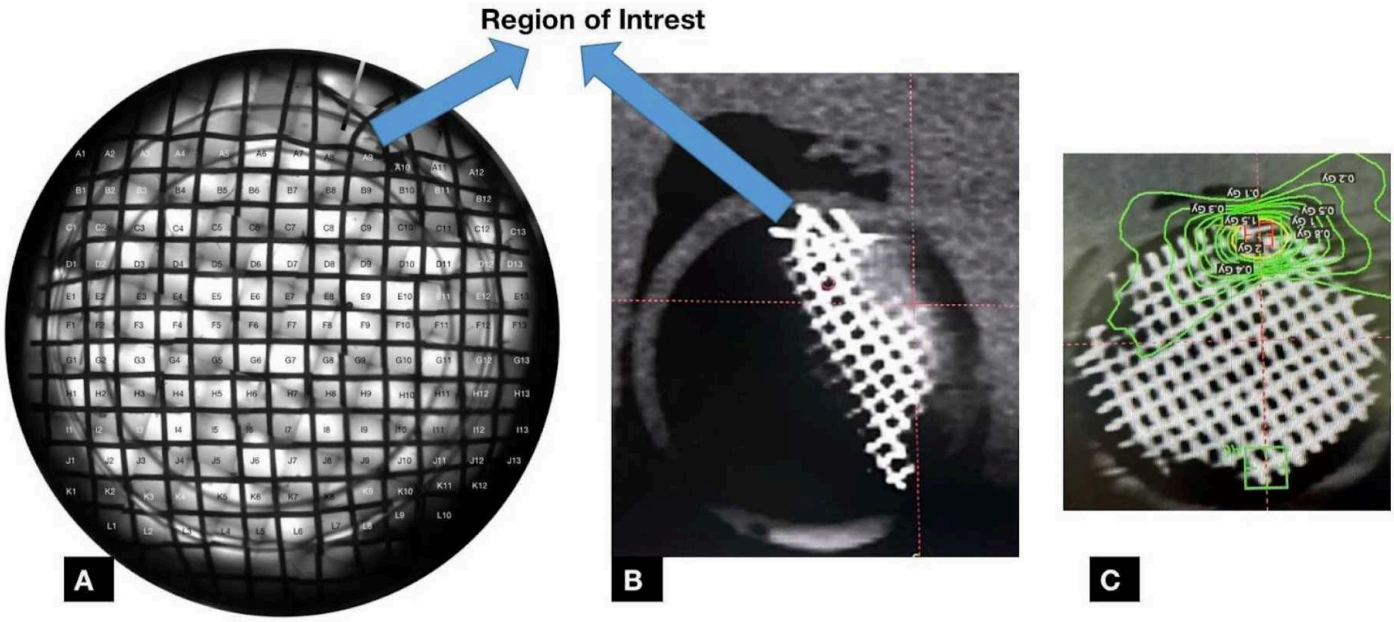


Figure 1

Localization of the region of interest and radiation dose mapping using the metal grid reference system. (A) Confocal microscopy image of the metal grid at 5× magnification, showing the grid structure used as a spatial reference for identifying the region of interest (ROI) during imaging. (B) Cone-beam computed tomography (CBCT) image of the grid embedded in the phantom, demonstrating localization of the ROI within the stereotactic coordinate system of the Gamma Knife. (C) Radiation dose distribution overlaid on the grid, illustrating the planned dose lines corresponding to the targeted irradiation region within the grid framework.

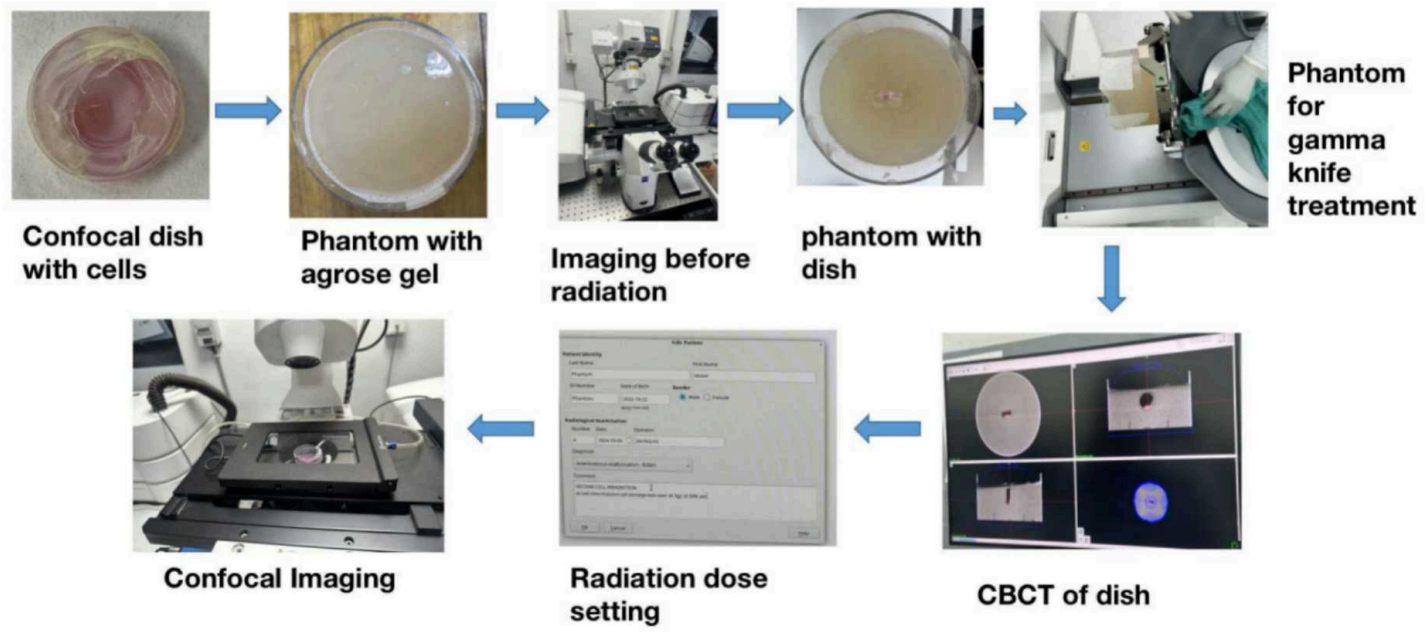


Figure 2

Experimental workflow for combining Gamma Knife irradiation with live confocal imaging of cultured cells. The procedure begins with culturing cells in a glass-bottom confocal dish, followed by preparation of an agarose-based phantom to mimic tissue conditions. The cells are first imaged by confocal microscopy prior to radiation exposure to record baseline morphology. The confocal dish is then embedded within the agarose phantom, creating a stable platform for stereotactic targeting. The phantom containing the dish is mounted onto the Gamma Knife stereotactic frame and positioned for treatment. A cone-beam computed tomography (CBCT) scan is performed to localize the dish within the phantom and enable accurate treatment planning. Based on the CBCT images, radiation dose parameters are defined in the Gamma Knife planning system. Following dose planning, targeted Gamma Knife irradiation is delivered to the cells within the phantom. After irradiation, the dish is removed and confocal microscopy is performed again to evaluate radiation-induced cellular responses, including morphological and functional changes.

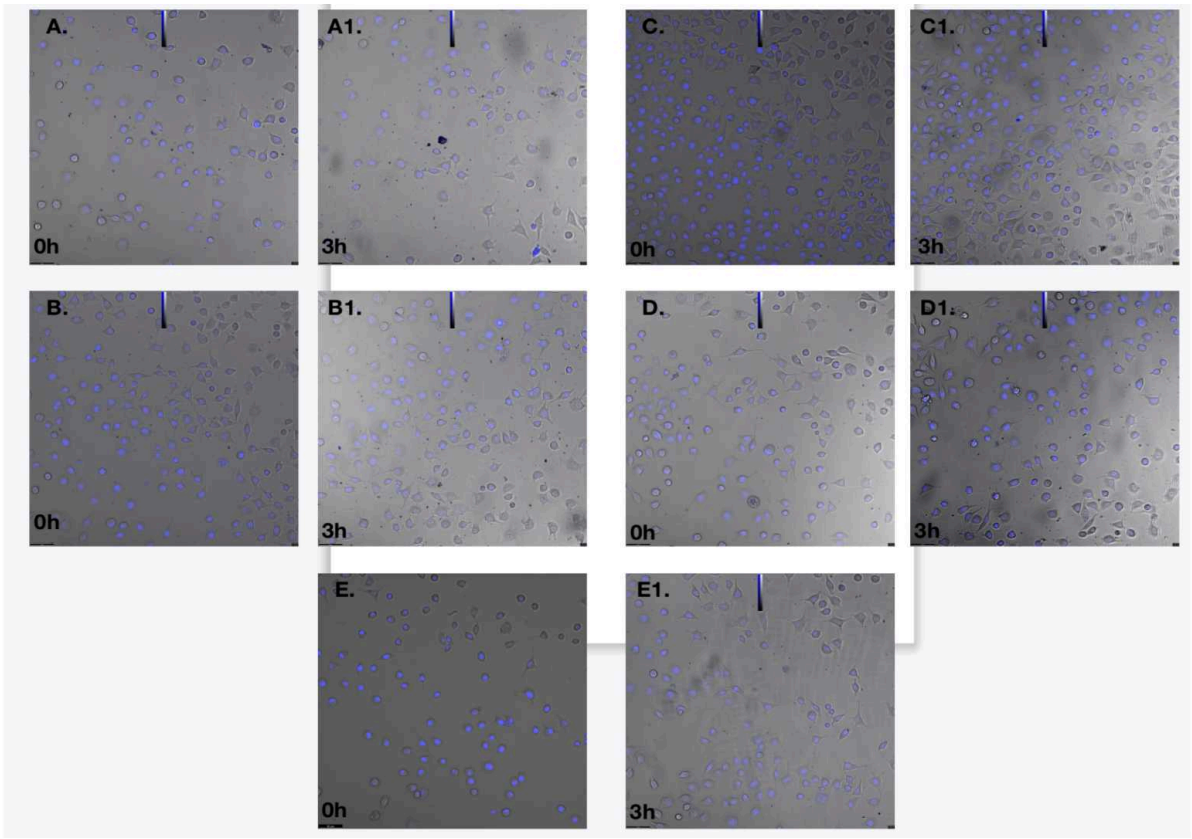


Figure 3

Representative confocal fluorescence micrographs of U-87 MG cells (nuclei stained with Hoechst, blue) following Gamma Knife stereotactic radiosurgery at different radiation doses. Panels A–E represent images acquired immediately after irradiation, while corresponding panels A1–E1 represent images at 3 hours post-irradiation. A/A1: 2.5 Gy, B/B1: 2.0 Gy, C/C1: 1.5 Gy, D/D1: 0.8 Gy, and E/E1: 0.5 Gy). At higher doses (2.5 Gy), a marked reduction in intact nuclei and increased cellular fragmentation are observed. Intermediate doses (1.0 Gy and 0.8 Gy) show prominent mitotic figures and increased cell density, indicating altered cell-cycle dynamics. Lower dose (0.5 Gy) demonstrates morphology closer to control conditions. These images illustrate dose- and time-dependent effects of radiation on cellular morphology and proliferation. Scale bar = 50 μm.